

Dual quark condensate in the Polyakov-loop extended Nambu–Jona-Lasinio model

Kouji Kashiwa,^{1,*} Hiroaki Kouno,^{2,†} and Masanobu Yahiro^{1,‡}

¹*Department of Physics, Graduate School of Sciences, Kyushu University, Fukuoka 812-8581, Japan*

²*Department of Physics, Saga University, Saga 840-8502, Japan*

(Dated: September 9, 2021)

The dual quark condensate $\Sigma^{(n)}$ proposed recently as a new order parameter of the spontaneous breaking of the \mathbb{Z}_3 symmetry are evaluated by the Polyakov-loop extended Nambu–Jona-Lasinio model, where n are winding numbers. The Polyakov-loop extended Nambu–Jona-Lasinio model well reproduces lattice QCD data on $\Sigma^{(1)}$ measured very lately. The dual quark condensate $\Sigma^{(n)}$ at higher temperatures is sensitive to the strength of the vector-type four-quark interaction in the Polyakov-loop extended Nambu–Jona-Lasinio model and hence a good quantity to determine the strength.

PACS numbers: 11.30.Rd, 12.40.-y

Recently, a new order parameter of the \mathbb{Z}_3 center symmetry was proposed by using the chiral condensate σ and evaluated by quenched [1, 2] and full lattice QCD [3]; the new order parameter is called *the dual quark condensate*. This makes it possible to discuss the connection between the quark confinement and the chiral symmetry. The relation can be discussed also by the Polyakov-loop extended NJL (PNJL) model [4] in which the Polyakov loop Φ is approximately treated as a classical variable. Actually, extensive studies are made on the relation; for example, see Refs. [4, 5, 6, 7, 8, 9, 10, 11, 12, 13, 14, 15]. The dual quark condensate is calculated also in the color $SU(2)$ system by the Dyson-Schwinger equation [16], but this approach does not treat the confinement mechanism dynamically. Very recently, the functional renormalization-group method was also applied to evaluate the dual quark condensate in the color $SU(3)$ system [17].

In this paper, we evaluate the dual quark condensate by using the PNJL model and show that the PNJL result can reproduce full lattice QCD (LQCD) data [3] on the dual quark condensate.

We consider the quark field q that obeys a twisted temporal boundary condition

$$q(\mathbf{x}, \beta) = e^{-i\varphi} q(\mathbf{x}, 0), \quad (1)$$

where φ is a twisted angle. Now we define the φ -dependent chiral condensate [1, 2, 3] by

$$\sigma(\varphi) = -\frac{1}{V} \langle \text{Tr}[(m + D_\varphi)^{-1}] \rangle, \quad (2)$$

where the twisted boundary condition (1) is imposed on the Dirac operator D_φ , but the bracket $\langle \dots \rangle$ keeps the anti-periodic boundary condition $\varphi = \pi$ [1, 2, 3]. The dual quark condensate $\Sigma^{(n)}$ is defined by

$$\Sigma^{(n)} = -\int_0^{2\pi} \frac{d\varphi}{2\pi} e^{-in\varphi} \sigma(\varphi) \quad (3)$$

with winding numbers n [1, 2, 3]. In particular, $\Sigma^{(1)}$ is called *the dressed Polyakov loop*. The winding number is 1 in both $\Sigma^{(1)}$ and Φ . In full LQCD calculations of Ref [3], the dressed Polyakov-loop is evaluated with $m/T = 0.032$. We can expect that the two have similar T dependence to each other. Thus, the dual quark condensate relates the chiral condensate to the quark confinement [1, 2, 3, 16, 17, 18].

We start with the two-flavor PNJL Lagrangian with the vector-type four-quark and the scalar-type eight-quark interactions; see Ref. [8] for the details. The scalar-type eight-quark interaction makes the chiral phase transition stronger. Hence, the PNJL result becomes consistent with LQCD data at finite T [8, 10, 19]. Furthermore, both the scalar-type eight-quark and the vector-type four-quark interaction are necessary for the PNJL model to reproduce LQCD data [20, 21, 22] at imaginary chemical potential [10].

Making the mean field approximation to the PNJL Lagrangian and performing the path integration of the resultant partition function over q under the twisted boundary condition (1), one can obtain the thermodynamical potential

$$\begin{aligned} \Omega = & -2N_f \int_A \frac{d^3p}{(2\pi)^3} \left[3E_p \right. \\ & + \frac{1}{\beta} \ln [1 + 3(\Phi + \bar{\Phi} e^{-\beta E_p^-}) e^{-\beta E_p^-} + e^{-3\beta E_p^-}] \\ & + \frac{1}{\beta} \ln [1 + 3(\bar{\Phi} + \Phi e^{-\beta E_p^+}) e^{-\beta E_p^+} + e^{-3\beta E_p^+}] \\ & \left. + G_s \sigma^2 - G_v \omega^2 + 3G_{s8} \sigma^4 + \mathcal{U}, \right] \quad (4) \end{aligned}$$

where $\sigma = \langle \bar{q}q \rangle$, $\omega = \langle \bar{q}\gamma_0 q \rangle$ and $E_p^\pm = E_p \pm iT\theta_\varphi$ with $E_p = \sqrt{\mathbf{p}^2 + M^2}$, $M = m_0 - 2G_s\sigma - 4G_{s8}\sigma^3$ and $iT\theta_\varphi = -2G_v\omega - i\pi T + iT\varphi$. Here, m_0 is the current quark mass and we use $m_0 = 5.5$ MeV. The constants G_s , G_v , G_{s8} denote coupling strengths of the scalar-type four-quark, the vector-type four-quark and the scalar-type eight-quark interaction, respectively. The Polyakov-loop potential \mathcal{U} is a function of Φ and its Hermitian conjugate $\bar{\Phi}$. The 3-dimensional momentum integration is regularized by a cutoff Λ . The classical variables $X = \sigma, \omega, \Phi, \bar{\Phi}$ are determined by solving the stationary conditions $\partial\Omega/\partial X = 0$ numerically, and $\Sigma^{(n)}$ is obtained numerically from $\sigma(\varphi)$ with (3). Details of the PNJL model are shown in Ref. [8].

*kashiwa@phys.kyushu-u.ac.jp

†kounoh@cc.saga-u.ac.jp

‡yahiro@phys.kyushu-u.ac.jp

In the PNJL calculations, two types of \mathcal{U} are often used; one has the polynomial form [5] and the other has the logarithm form [6]. The former (latter) potential is referred to as RTW05 (RRW06). Parameters of these potentials are fitted to LQCD data at finite T in the pure gauge limit [23, 24], but one of the parameters, T_0 , is usually refitted to reproduce the pseudo-critical temperature $T_c = 173 \pm 8$ MeV in full LQCD [25]. The value of T_0 thus determined is 185 (200 MeV) for the RTW05 (RRW06) potential. The RRW06 potential can reproduce LQCD data [20, 21, 22] at imaginary chemical potential, but the RTW05 does not [10]. Therefore, the RRW06 potential is mainly used in the present PNJL analyses.

We do four types of PNJL calculations shown in Table I. In PNJL-I, G_s and Λ are adjusted to the pion mass $M_\pi = 138$ MeV and the pion decay constant and $f_\pi = 93.3$ MeV at $T = 0$; see Ref. [8] for values of the parameters. In PNJL-II, -III and -IV, G_s , G_{s8} , Λ are fitted to $M_\pi = 138$ MeV and $f_\pi = 93.3$ MeV and the sigma meson mass $M_\sigma = 600$ MeV; see Ref. [8] for values of the parameters. Since the empirical value of M_σ has a large error bar, the empirical value is not a strong constraint to determine the strength G_{s8} . We then think G_{s8} as a nearly-free parameter. The value of G_{s8} determined above is just an example. In PNJL-III, the vector-type interaction is a free parameter. The strength of the vector-type interaction was determined to reproduce LQCD data [20, 21, 22] at imaginary chemical potential [10]. The ratio G_v/G_s is 0.85. As an example, we take a bit smaller value of $G_v/G_s = 0.667$. For comparison, we also do the NJL calculation with the scalar-type eight-quark interaction; this is referred to as NJL. Since NJL agrees with PNJL-II in the limit of $T = 0$ [9], the same parameter set is taken in the two models.

Model	Interaction	\mathcal{U}	T_c^Φ	T_c^σ	$T_c^{\Sigma^{(1)}}$	line
PNJL-I	σ^2	RRW06	$1.01T_c$	$1.32T_c$	$1.01T_c$	thin-solid
PNJL-II	σ^2, σ^4	RRW06	T_c	$1.14T_c$	T_c	solid
PNJL-III	$\sigma^2, \sigma^4, \omega^2$	RRW06	T_c	$1.14T_c$	T_c	dashed
PNJL-IV	σ^2, σ^4	RTW05	$0.98T_c$	$1.10T_c$	$1.11T_c$	dotted
NJL	σ^2, σ^4	-	-	$0.94T_c$	$0.97T_c$	dot-dashed

TABLE I: Definitions and results of PNJL and NJL calculations. Symbols, RTW05 and RRW06, are the Polyakov potentials of polynomial type [5] and logarithm type [6], respectively, while $\sigma^2, \sigma^4, \omega^2$ denote the scalar-type four-quark, the scalar-type eight-quark and the vector-type four-quark interaction, respectively. Symbols $T_c^\sigma, T_c^\Phi, T_c^{\Sigma^{(1)}}$ denote the pseudo-critical temperatures defined by peak positions of $d\sigma/dT, d\Phi/dT, d\Sigma^{(1)}/dT$, respectively. Here, $T_c = 173$ MeV.

As mentioned above, the twisted boundary condition (1) is imposed on D_φ . Therefore, Φ and $\bar{\Phi}$ are first obtained under the anti-periodic boundary condition $\varphi = \pi$. The quantities $\sigma(\varphi)$ and $\omega(\varphi)$ are determined by solving the stationary conditions, $\partial\Omega/\partial\sigma = 0$ and $\partial\Omega/\partial\omega = 0$, numerically under the twisted boundary condition (1) with Φ and $\bar{\Phi}$ fixed to the values determined at $\varphi = \pi$.

The pseudo-critical temperature T_c^Φ of the deconfinement

crossover is usually defined by a peak position of either the Polyakov-loop susceptibility or $d\Phi/dT$. In the present analysis, we take the latter to compare T_c^Φ with the pseudo-critical temperature $T_c^{\Sigma^{(1)}}$ estimated by a peak position of $d\Sigma^{(1)}/dT$, because we can not define the susceptibility for the dressed Polyakov loop $\Sigma^{(1)}$. For consistency, the pseudo-critical temperature T_c^σ of the chiral crossover is defined by a peak position of $d\sigma/dT$. In the PNJL calculations with the RRW06 potential, $d\sigma/dT$ has two peaks, but we take the second peak close to a peak position of the chiral susceptibility.

Table I summarizes values of $T_c^\Phi, T_c^\sigma, T_c^{\Sigma^{(1)}}$ in five types of model calculations, where the values are normalized by $T_c = 173$ MeV, i.e. the LQCD result [25] for T_c^Φ and T_c^σ . In PNJL-I, -II, -III with the RRW06 potential, T_c^Φ and $T_c^{\Sigma^{(1)}}$ are close to each other and also to the LQCD data [25], although this property is not seen in PNJL-IV with the RTW05 potential. As for T_c^σ , PNJL-II is more consistent with the LQCD data than PNJL-I and hence the scalar-type eight-quark interaction is necessary to reproduce the LQCD data.

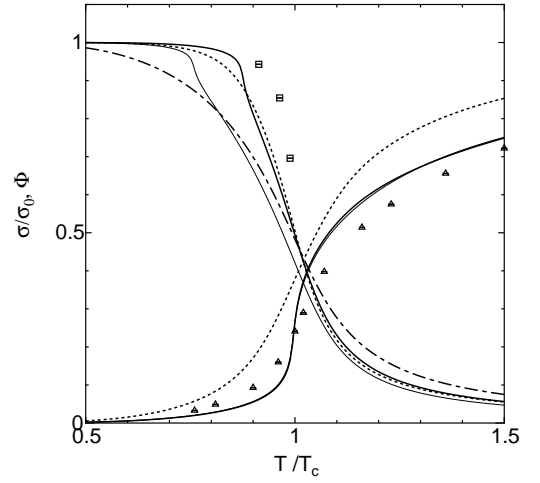


Fig. 1: Chiral condensate as a function of T/T_c^σ and renormalized Polyakov loop as a function of T/T_c^Φ in the case of $\varphi = \pi$. Here, σ is normalized by the value σ_0 at $T = 0$. The values of T_c^σ and T_c^Φ are summarized in Table. I. Definitions of lines are also shown in Table. I. LQCD data shown by box and triangle symbols are taken from Ref. [26] and Ref. [27], respectively.

Figure 1 presents T -dependence of the chiral condensate and that of renormalized Φ , where the anti-periodic boundary condition $\varphi = \pi$ is taken. The resultant chiral condensate σ is normalized by the value σ_0 at $T = 0$. Temperature T is normalized by T_c^σ for the chiral condensate and by T_c^Φ for renormalized Φ to compare the shapes of σ/σ_0 and Φ with LQCD data [26, 27]. Also for the shape for σ , PNJL-II (solid curve) gives a better agreement with the LQCD data than PNJL-I (thin solid curve). Meanwhile, the solid and thin solid curves are almost identical for Φ , indicating that the scalar-type eight-quark interaction hardly affects the shape of Φ . At zero quark chemical potential, the vector-type four-quark interaction does not affect σ and Φ in the mean field approximation; hence, PNJL-III yields the same σ and Φ as PNJL-II

in Fig. 1. Nevertheless, the interaction gives a sizable effect on $\Sigma^{(1)}$, as shown later. For the shape of Φ , PNJL-IV (dotted curve) gives a larger disagreement with the LQCD data than PNJL-II. Thus, the RRW06 potential is better than the RTW05 potential also for the shape of Φ .

Full LQCD simulation of Ref. [3] shows that $T_c^{\Sigma^{(1)}} \simeq T_c^\sigma \simeq T_c^\Phi \simeq 153$ MeV, while that of Ref. [25] does $T_c^\sigma \simeq T_c^\Phi \simeq 173$ MeV. The two LQCD results have a systematic error of $\sim 10\%$. Moreover, it is reported in Ref. [28] for the $2+1$ -flavor system that there exists a non-negligible deviation between T_c^σ and T_c^Φ . This indicates that it is an unsettled problem whether T_c^σ and T_c^Φ really coincide or not. In this work, however, we assume the coincidence, since the LQCD data [3] that we are analyzing has the property. In the present analysis, temperature is normalized by T_c , but it is taken to be 153 MeV for LQCD data of Ref. [3] and 173 MeV for model calculations and LQCD data of Ref. [25, 26, 27].

Figure 2 presents the normalized dressed Polyakov loop $\Sigma^{(1)}/\Sigma_{T_c}^{(1)}$ as a function of $T/T_c^{\Sigma^{(1)}}$, where $\Sigma_{T_c}^{(1)}$ is the dressed Polyakov loop at $T = T_c^{\Sigma^{(1)}}$. PNJL-I (thin solid line) and PNJL-II (solid line) well reproduces LQCD data [3] (box symbols), but PNJL-IV (dotted line) and NJL (dot-dashed line) do not. Near $T_c^{\Sigma^{(1)}}$, the scalar-type eight-quark interaction hardly affects the dressed Polyakov loop. Thus, the RRW06 potential is necessary to explain T dependence of Φ , σ and $\Sigma^{(1)}$ consistently.

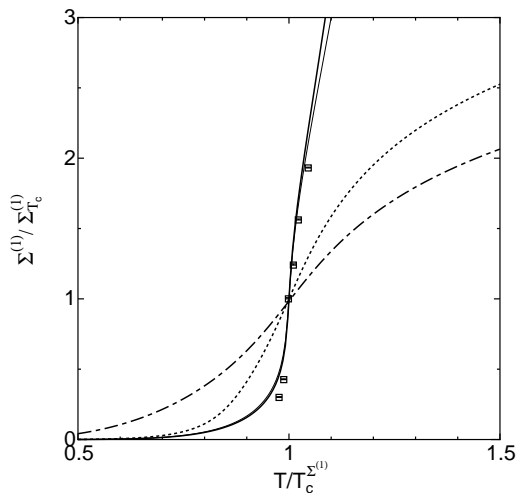


Fig. 2: Normalized dressed Polyakov loop as a function of $T/T_c^{\Sigma^{(1)}}$. Definitions of lines are shown in Table. I. LQCD data (box symbols) are taken from Ref. [3].

Figure 3 shows φ -dependence of σ at $T = 200$ and 250 MeV, while Fig. 4 represented T -dependence of the dual quark condensates with $n = 0$ and 1. The difference between PNJL-I (thin-solid line) and PNJL-II (solid line) shows an effect of the scalar-type eight-quark interaction. As shown in Fig. 3, the effect on σ is large around $\varphi = \pi$, but small around $\varphi = 0$. The absolute value of σ is relatively larger around $\varphi = 0$. As a consequence, as shown in Fig. 4, the effect on

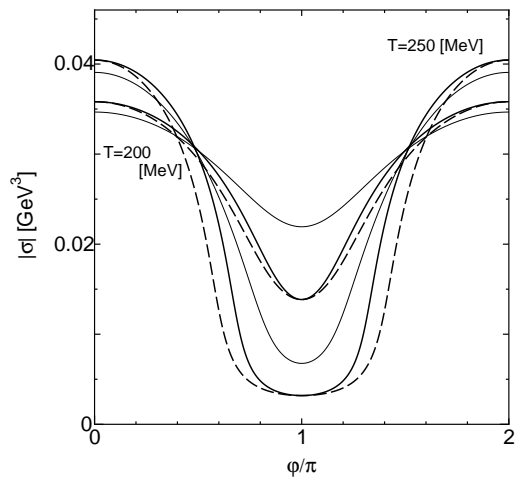


Fig. 3: φ -dependence of the chiral condensate at $T = 200$ and 250 MeV. Definitions of lines are shown in Table. I.

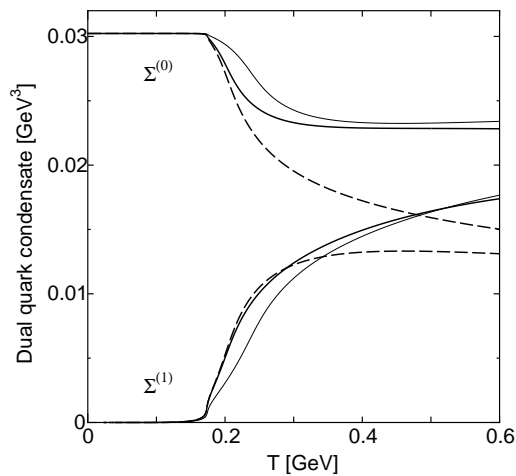


Fig. 4: T -dependence of the dual quark condensate. Definitions of lines are shown in Table. I.

$\Sigma^{(0)}$ and $\Sigma^{(1)}$ are appreciable only at $T_c^{\Sigma^{(1)}} < T < 2T_c^{\Sigma^{(1)}}$. Thus, the effect of the eight-quark interaction becomes more appreciable for σ at $\varphi = \pi$ than for $\Sigma^{(0)}$ and $\Sigma^{(1)}$. At $T > 2T_c^{\Sigma^{(1)}}$, the effect becomes negligible, since σ itself is tiny there. Meanwhile, the difference between PNJL-II (solid line) and PNJL-III (dashed line) presents an effect of the vector-type four-quark interaction. The effect on σ is zero at $\varphi = \pi$, and appreciable at nonzero $\varphi (\neq \pi)$, as shown in Fig. 3. The effect on $\Sigma^{(0)}$ and $\Sigma^{(1)}$ is then appreciable at $T_c^{\Sigma^{(1)}} < T < 1.5T_c^{\Sigma^{(1)}}$ and sizable at $T > 1.5T_c^{\Sigma^{(1)}}$, as shown in Fig. 4. Thus, the effect of the vector-type four-quark interaction becomes more appreciable for $\Sigma^{(0)}$ and $\Sigma^{(1)}$ than for σ at $\varphi = \pi$. This indicates that the dual quark condensate at $T > 1.5T_c^{\Sigma^{(1)}}$ is a good quantity to determine the strength of the vector-type four-quark interaction.

The present PNJL results are consistent with the LQCD

data for $\Sigma^{(1)}/\Sigma_{T_c}^{(1)}$ near T_c , but not for $\sigma(\varphi)$ itself even if both are compared at the same values of $T/T_c^{\Sigma^{(1)}}$, although the latter is not shown explicitly in this paper. In LQCD, $\sigma(\varphi)$ and $\Sigma^{(1)}$ are not renormalized, while Φ presented in Fig. 1 is renormalized. The reasonable agreement of the PNJL result with the LQCD one for σ/σ_0 and Φ in Fig. 1 and $\Sigma^{(1)}/\Sigma_{T_c}^{(1)}$ in Fig. 2 may imply that σ/σ_0 and $\Sigma^{(1)}/\Sigma_{T_c}^{(1)}$ have better renormalization properties than $\sigma(\varphi)$ itself.

Finally, we discuss the sensitivity of $\Sigma^{(1)}$ to the parameters of the PNJL model. If Λ is varied by 10 %, the pion decay constant at $T = 0$ is changed by about 20 %. Hence, one can

change Λ by only 0.1 % in order that the calculated pion decay constant is consistent with the observed one with 0.1 % error. This is also the case for G_s . If Λ and G_s are varied by 1 %, $\Sigma^{(1)}$ are changed by about 10 %, but the normalized quantity $\Sigma^{(1)}/\Sigma_{T_c}^{(1)}$ is hardly changed near T_c . Further, $\Sigma^{(1)}$ near T_c is much less sensitive to G_{s8} and G_v , although these are nearly-free parameters. Thus, we can think that $\Sigma^{(1)}/\Sigma_{T_c}^{(1)}$ near T_c changes little from the present values.

K.K. is supported by the Japan Society for the Promotion of Science for Young Scientists.

-
- [1] E. Bilgici, F. Bruckmann, C. Gatttringer, and C. Hagen, Phys. Rev. D **77**, 094007 (2008).
- [2] F. Bruckmann, C. Hagen, E. Bilgici, and C. Gatttringer, Pos **Lattice2008**, 262 (2008); Pos **Confinement8**, 054 (2008).
- [3] E. Bilgici, F. Bruckmann, J. Danzer, C. Gatttringer, C. Hagen, E. M. Ilgenfritz, and A. Maas, arXiv:0906.3957; E. Bilgici, PhD Thesis, University of Graz, Austria, 2009 (<http://physik.uni-graz.at/itp/files/bilgici/dissertation.pdf>).
- [4] K. Fukushima, Phys. Lett. B **591**, 277 (2004); Phys. Rev. D **77**, 114028 (2008); Phys. Rev. D **78**, 114019 (2008).
- [5] C. Ratti, M. A. Thaler, and W. Weise, Phys. Rev. D **73**, 014019 (2006).
- [6] S. Rößner, C. Ratti, and W. Weise, Phys. Rev. D **75**, 034007 (2007).
- [7] P. Costa, M. C. Ruivo, C. A. de Sousa, H. Hansen, and W. M. Alberico, Phys. Rev. D **79**, 116003 (2009).
- [8] K. Kashiwa, H. Kouno, M. Matsuzaki, and M. Yahiro, Phys. Lett. B **662**, 26 (2008); K. Kashiwa, M. Matsuzaki, H. Kouno, Y. Sakai, and M. Yahiro, Phys. Rev. D **79**, 076008 (2009).
- [9] Y. Sakai, K. Kashiwa, H. Kouno, and M. Yahiro, Phys. Rev. D **77**, 051901(R) (2008); Phys. Rev. D **78**, 036001 (2008); Y. Sakai, K. Kashiwa, H. Kouno, M. Matsuzaki, and M. Yahiro, Phys. Rev. D **78**, 076007 (2008).
- [10] Y. Sakai, K. Kashiwa, H. Kouno, M. Matsuzaki, and M. Yahiro, Phys. Rev. D **79**, 096001 (2009).
- [11] H. Abuki, R. Anglani, R. Gatto, G. Nardulli, and M. Ruggieri, Phys. Rev. D **78**, 034034 (2008); H. Abuki, M. Ciminale, R. Gatto, and M. Ruggieri, Phys. Rev. D **79**, 034021 (2009).
- [12] T. Hell, S. Rößner, M. Cristoforetti, and W. Weise, Phys. Rev. D **79**, 014022 (2009).
- [13] K. Kashiwa, M. Yahiro, H. Kouno, M. Matsuzaki, and Y. Sakai, J. Phys. G **36**, 105001 (2009).
- [14] H. Kouno, Y. Sakai, K. Kashiwa, and M. Yahiro, J. Phys. G **36**, 115010 (2009).
- [15] S. i. Nam, arXiv:hep-ph/0905.3609.
- [16] C. S. Fischer, Phys. Rev. Lett **103**, 052003 (2009); C. S. Fischer, and J. A. Mueller, Phys. Rev. D **80**, 074029 (2009).
- [17] J. Braun, L. M. Haas, F. Marhauser, and J. M. Pawłowski, arXiv:hep-ph/0908.0008.
- [18] F. Synatschke, A. Wipf, and K. Langfeld, Phys. Rev. D **77**, 114018 (2008).
- [19] K. Kashiwa, H. Kouno, T. Sakaguchi, M. Matsuzaki, and M. Yahiro, Phys. Lett. B **647**, 446 (2007).
- [20] P. de Forcrand and O. Philipsen, Nucl. Phys. **B642**, 290 (2002); Nucl. Phys. **B673**, 170 (2003).
- [21] M. D'Elia and M. P. Lombardo, Phys. Rev. D **67**, 014505 (2003); Phys. Rev. D **70**, 074509 (2004); M. D'Elia, F. Di Renzo and M. P. Lombardo, Phys. Rev. D **76**, 114509 (2007).
- [22] H. S. Chen and X. Q. Luo, Phys. Rev. D **72**, 034504 (2005); arXiv:hep-lat/0702025; L. K. Wu, X. Q. Luo, and H. S. Chen, Phys. Rev. D **76**, 034505 (2007).
- [23] G. Boyd, J. Engels, F. Karsch, E. Laermann, C. Legeland, M. Lütgemeier, and B. Petersson, Nucl. Phys. **B469**, 419 (1996).
- [24] O. Kaczmarek, F. Karsch, P. Petreczky, and F. Zantow, Phys. Lett. B **543**, 41 (2002).
- [25] F. Karsch, E. Laermann, and A. Peikert, Nucl. Phys. **B605**, 579 (2001).
- [26] G. Boyd, S. Gupta, F. Karsch, E. Laermann, B. Petersson, and K. Redlich, Phys. Lett. B **349**, 170 (1995).
- [27] O. Kaczmarek, and F. Zantow, Phys. Rev. D **71**, 114510 (2005).
- [28] Y. Aoki, Z. Fodor, S. D. Katz, and K. K. Szabó, Phys. Lett. B **643**, 46 (2006).